Precoded Massive MU-MIMO Uplink Transmission under Transceiver I/Q Imbalance

Aki Hakkarainen*, Janis Werner*, Kapil R. Dandekar† and Mikko Valkama*
*Department of Electronics and Communications Engineering, Tampere University of Technology, Tampere, Finland
Email: {aki.hakkarainen, janis.werner, mikko.e.valkama}@tut.fi
†Department of Electrical and Computer Engineering, Drexel University, Philadelphia, PA, USA
Email: dandekar@coe.drexel.edu

***Abstract*—In massive multiple-input multiple-output (MIMO) systems, combined with digital array processing, the amount of the associated radio frequency (RF) front-ends is inevitably high. This paper addresses how imperfections in these RF front-ends affect the overall system performance in precoded massive multi-user MIMO (MU-MIMO) uplink transmission. In particular, we focus on transceiver in-phase/quadrature (I/Q) imbalances and their mitigation with RF-aware spatial processing. We first derive the essential distortion and interference models for OFDMA-based massive MU-MIMO uplink system under I/Q imbalances, and then propose augmented spatial post-processing to be carried out in the uplink receiver (RX) for mitigating the harmful effects efficiently. Numerical examples show that the augmented spatial RX processing clearly outperforms the conventional linear processing, and thus provides significant performance improvements with practical low-cost RF front-ends.**

***Index Terms*—antenna arrays, in-phase/quadrature (I/Q) imbalance, interference suppression, massive multi-user multiple-input multiple-output (MU-MIMO), orthogonal frequency-division multiple access (OFDMA)**

I. Introduction

Massive multiple-input multiple-output (MIMO) systems consist of tens or even hundreds of antennas [1]. Consequently, the amount of the associated radio frequency (RF) front-ends is very high, especially when emphasizing digital array processing and beamforming. In order to implement cost-effective and reasonable size massive MIMO devices in practice, the size and cost of individual RF transceivers should be low. Unfortunately, this requirement may easily result in performance degradation due to imperfections in the RF components [1], [2].

RF imperfections in massive MIMO systems have gained increasing interest recently. Our earlier work in [3] showed that RF imperfections in massive antenna arrays significantly degrade the system performance and can actually result in even bigger problems than in MIMO systems with fewer antennas. In [4], the effects of oscillator phase noise on uplink massive multiuser MIMO (MU-MIMO) systems are studied and the imperfection is shown to degrade the overall link performance. In [5], multiple aspects of the RF imperfections are provided in terms of energy efficiency as well as estimation and capacity limits in massive MIMO systems. The impact of RF imperfections is modeled in [5] as a residual additive Gaussian noise which depends only on the signal power. While such model may hold for the residual RF imperfections after the actual RF impairment processing, it does not take into account the inherent structure of distortion mechanisms of different RF imperfections.

In this paper, we consider and emphasize the structure of certain imperfections in the associated RF front-ends in massive MIMO systems. Especially, we focus on in-phase/quadrature (I/Q) imbalance and its mitigation jointly within spatial receiver (RX) post-processing without a need for separate I/Q imbalance mitigation or calibration. Starting from I/Q imbalance modeling in uplink orthogonal frequency division multiple access (OFDMA) based massive MU-MIMO systems, we show that I/Q imbalance in the RF front-ends causes signal distortion where each subcarrier signal is interfered by the signals at the image subcarrier, implying hence inter-user interference. Stemming from this phenomenon and based on the earlier I/Q imbalance studies in [6]–[9], we exploit the so-called augmented spatial post-processing at RX, now taking into account the effects of precoding in uplink transmitters (TXs). We derive the minimum mean-square error (MMSE)-optimal augmented spatial post-processing solution, and by simulating the system performance as a funtion of multiple system parameters, we show that the proposed solution outperforms the traditional per-subcarrier processing clearly and thus provides significant performance improvements without costly changes in the associated RF front-ends.

This paper is organized as follows. Section II introduces fundamental signal and system models as well as RX post-processing principles in base station (BS). In Section III, we present the RF-aware precoding method as well as the linear and augmented linear MMSE (LMMSE) post-processing solutions. In Section IV, we provide numerical examples in terms of the signal-to-interference-plus-noise ratio (SINR). Finally, the conclusions are drawn in Section V.

Notation: Vectors and matrices are written with bold characters. The superscripts $(\cdot)^T$, $(\cdot)^H$, $(\cdot)^*$ and $(\cdot)^{-1}$ represent

This work was supported by the Finnish Funding Agency for Technology and Innovation (Tekes) under the project "Reconfigurable Antenna-based Enhancement of Dynamic Spectrum Access Algorithms", the Industrial Research Fund of Tampere University of Technology (Tuula and Yrjö Neuvo Fund), the Academy of Finland under the project 251138 "Digitally-Enhanced RF for Cognitive Radio Devices", the Doctoral Programme of the President of Tampere University of Technology, and the Foundation of Nokia Corporation.
The work was also supported by National Science Foundation (NSF) under award number 1147838.

978-1-4799-7470-2/14/$31.00 ©2014 IEEE

transpose, Hermitian (conjugate) transpose, complex conjugate and matrix inverse, respectively. The tilde sign $\widetilde{(\cdot)}$ is used to present an augmented quantity and the results obtained by augmented processing. We write $\mathrm{diag}\,(x_{11}, x_{22}, \cdots, x_{ii})$ to denote the diagonal matrix $\mathbf{X}$ with elements x_{ii} on the main diagonal. The statistical expectation is denoted with $\mathbb{E}\,[\cdot]$. Finally, $\mathrm{tr}\,(\cdot)$ denotes the trace of a matrix.

II. Signal and System Models

In this paper, we consider precoded spatial multiplexing in uplink OFDMA MU-MIMO transmission from an arbitrary subcarrier point of view. Our generic model comprises a single BS which serves simultaneously multiple user equipment (UEs) in each time-frequency resource. The subcarriers are indexed with $c \in \{-C/2, \ldots, -1, 1, \ldots, C/2\}$ where C is the total amount of active subcarriers. Furthermore, the image (or mirror) subcarrier is defined as $c' = -c$. With U and V we denote the number of UEs spatially multiplexed at subcarriers c and c', respectively. The corresponding UEs are indexed with $u \in \{1, \ldots, U\}$ and $v \in \{1, \ldots, V\}$. Note that depending on the frequency allocation for the UEs, u and v might refer to the same UE which is active at both subcarriers c and c'.

The BS has N RX antennas whereas UE u is equipped with M_u TX antennas. The number of parallel independent data streams of UE u at subcarrier c is denoted by Q_u. At subcarrier c, the data symbol vector $\mathbf{x}_{u,c} \in \mathbb{C}^{Q_u \times 1}$ of UE u is precoded with precoder $\mathbf{G}_{u,c} \in \mathbb{C}^{M_u \times Q_u}$ resulting in antenna signal vector $\mathbf{s}_{u,c} \in \mathbb{C}^{M_u \times 1}$. The corresponding variables at the image subcarrier c' for UE v are denoted by $\mathbf{x}_{v,c'} \in \mathbb{C}^{Q_v \times 1}$, $\mathbf{G}_{v,c'} \in \mathbb{C}^{M_v \times Q_v}$, and $\mathbf{s}_{v,c'} \in \mathbb{C}^{M_v \times 1}$. In addition to the UE signals, we include L external interferers into the model. External interferer l is assumed to have J_l TX antennas and the spatial signal snapshot vector originating from that external interferer is denoted by $\mathbf{s}_{\mathrm{int},l,c} \in \mathbb{C}^{J_l \times 1}$. All data vectors refer to subcarrier-level (frequency-domain) quantities in the considered OFDMA radio system, i.e., prior to the inverse fast Fourier transform (IFFT) in the TXs and after the fast Fourier transform (FFT) in the RXs.

A. Joint TX+RX I/Q Imbalances in MU-MIMO Systems

Direct-conversion transceivers (DCTs) [10] are regarded as promising candidates for the radio architecture in massive MIMO systems since they do not need additional intermediate-frequency filters, in contrast to the heterodyne transceivers [10]. Consequently, the total size and cost of DCT are smaller compared to conventional solutions. Unfortunately, the imperfections in the analog RF electronics of DCT are known to result in I/Q imbalance [10], [11]. I/Q imbalance is caused by gain and phase imbalance, g and ϕ, between the I and Q branches. The roots of the phenomenon lie in the implementation inaccuracies of the associated amplifiers, filters, mixers and digital-to-analog and analog-to-digital converters.

In precoded uplink MU-MIMO transmission, the transmitted antenna signal vector of UE u at subcarrier c, assuming first perfect I/Q matching, can be written as $\mathbf{s}_{u,c} = \mathbf{G}_{u,c}\mathbf{x}_{u,c}$ [12]. However, when considering *I/Q imbalance in the TX electronics of an individual UE*, the transmitted antenna signal vector of UE u at subcarrier c becomes [9], [13]

$$\begin{aligned}\mathbf{s}_{\mathrm{Txi},u,c} &= \mathbf{K}_{\mathrm{Tx1},u,c}\mathbf{s}_{u,c} + \mathbf{K}_{\mathrm{Tx2},u,c}\mathbf{s}^*_{u,c'} \\ &= \mathbf{K}_{\mathrm{Tx1},u,c}\mathbf{G}_{u,c}\mathbf{x}_{u,c} + \mathbf{K}_{\mathrm{Tx2},u,c}\mathbf{G}^*_{u,c'}\mathbf{x}^*_{u,c'} \end{aligned} \quad (1)$$

with the TX I/Q imbalance matrices $\mathbf{K}_{\mathrm{Tx1},u,c} = \mathrm{diag}(K_{\mathrm{Tx1},1,u,c}, \cdots, K_{\mathrm{Tx1},M_u,u,c}) \in \mathbb{C}^{M_u \times M_u}$ and $\mathbf{K}_{\mathrm{Tx2},u,c} = \mathrm{diag}(K_{\mathrm{Tx2},1,u,c}, \cdots, K_{\mathrm{Tx2},M_u,u,c}) \in \mathbb{C}^{M_u \times M_u}$. The diagonal entries of the matrices are given by $K_{\mathrm{Tx1},m,u,c} = (1 + g_{\mathrm{Tx},m,u,c}e^{j\phi_{\mathrm{Tx},m,u,c}})/2$ and $K_{\mathrm{Tx2},m,u,c} = (1 - g_{\mathrm{Tx},m,u,c}e^{j\phi_{\mathrm{Tx},m,u,c}})/2$ where $g_{\mathrm{Tx},m,u,c}$ and $\phi_{\mathrm{Tx},m,u,c}$ are the gain and phase imbalance coefficients for TX antenna branch m of user u at subcarrier c [11]. Clearly, the transmitted signal is distorted, resulting in cross-talk between subcarriers c and c'. This is a well-known phenomenon, discussed e.g. in [9], [11], [13]–[15]. In general, when the image subcarrier c' is allocated to another UE v, this results in cross-talk between UEs at mirror subcarriers.

The transmitted signal vectors propagate through the wireless channels and are then received in the RX. Consequently, the total received signal vector $\mathbf{r}_{\mathrm{Txi},c} \in \mathbb{C}^{N \times 1}$ at subcarrier c under I/Q imbalances of UE TXs is

$$\begin{aligned}\mathbf{r}_{\mathrm{Txi},c} = &\sum_{u=1}^{U} \mathbf{H}_{u,c}\mathbf{K}_{\mathrm{Tx1},u,c}\mathbf{G}_{u,c}\mathbf{x}_{u,c} \\ &+ \sum_{v=1}^{V} \mathbf{H}_{v,c}\mathbf{K}_{\mathrm{Tx2},v,c}\mathbf{G}^*_{v,c'}\mathbf{x}^*_{v,c'} + \mathbf{z}_c \end{aligned} \quad (2)$$

where we assume, for simplicity, perfect timing and frequency synchronization between the UEs and the BS. Here, $\mathbf{H}_{u,c} \in \mathbb{C}^{N \times M_u}$ and $\mathbf{H}_{v,c} \in \mathbb{C}^{N \times M_v}$ are the channel response matrices of UEs u and v, respectively, at subcarrier c. Throughout the paper, the channel response elements are assumed to be constant within each narrow subcarrier. Finally, the external interference plus noise vector $\mathbf{z}_c \in \mathbb{C}^{N \times 1}$ is given by

$$\mathbf{z}_c = \sum_{l=1}^{L} \mathbf{H}_{\mathrm{int},l,c}\mathbf{s}_{\mathrm{int},l,c} + \mathbf{n}_c. \quad (3)$$

Here, $\mathbf{H}_{\mathrm{int},l,c} \in \mathbb{C}^{N \times J_l}$ is the channel response matrix of external interferer l, and $\mathbf{n}_c \in \mathbb{C}^{N \times 1}$ models the additive noise in the RX electronics. Noise elements in different RX branches are assumed to be complex, circular and mutually uncorrelated. A corresponding formulation for the external interference and noise at the image subcarrier is obtained from (3) by substituting the subcarrier index c with c'.

When taking next into account that *I/Q imbalance occurs also in the RX*, the received signal vector $\mathbf{r}_{\mathrm{TxRxi},c} \in \mathbb{C}^{N \times 1}$ at subcarrier c under joint TX+RX I/Q imbalances is equal to

$$\begin{aligned}\mathbf{r}_{\mathrm{TxRxi},c} &= \mathbf{K}_{\mathrm{Rx1},c}\mathbf{r}_{\mathrm{Txi},c} + \mathbf{K}_{\mathrm{Rx2},c}\mathbf{r}^*_{\mathrm{Txi},c'} \\ &= \sum_{u=1}^{U} \widetilde{\mathbf{\Psi}}_{u,c}\mathbf{G}_{u,c}\mathbf{x}_{u,c} + \sum_{v=1}^{V} \widetilde{\mathbf{\Omega}}_{v,c}\mathbf{G}^*_{v,c'}\mathbf{x}^*_{v,c'} \\ &\quad + \mathbf{K}_{\mathrm{Rx1},c}\mathbf{z}_c + \mathbf{K}_{\mathrm{Rx2},c}\mathbf{z}^*_{c'} \end{aligned} \quad (4)$$

where the RX I/Q imbalance matrices are given by $\mathbf{K}_{\text{Rx1},c} = \text{diag}(K_{\text{Rx1},1,c}, \cdots, K_{\text{Rx1},N,c}) \in \mathbb{C}^{N\times N}$ and $\mathbf{K}_{\text{Rx2},c} = \text{diag}(K_{\text{Rx2},1,c}, \cdots, K_{\text{Rx2},N,c}) \in \mathbb{C}^{N\times N}$. Here, the diagonal entries of the matrices are given by $K_{\text{Rx1},n,c} = (1 + g_{\text{Rx},n,c}e^{-j\phi_{\text{Rx},n,c}})/2$ and $K_{\text{Rx2},n,c} = (1 - g_{\text{Rx},n,c}e^{j\phi_{\text{Rx},n,c}})/2$. Similarly as for the TX, $g_{\text{Rx},n,c}$ and $\phi_{\text{Rx},n,c}$ denote the gain and phase imbalance coefficients of RX antenna branch n [11]. Furthermore, the total effective channel matrices, consisting of the influence of TX and RX I/Q imbalances as well as the wireless propagation channels, are given by

$$\widetilde{\mathbf{\Psi}}_{u,c} = \begin{bmatrix}\mathbf{K}_{\text{Rx1},c} & \mathbf{K}_{\text{Rx2},c}\end{bmatrix}\begin{bmatrix}\mathbf{H}_{u,c} & \mathbf{0}\\ \mathbf{0} & \mathbf{H}^*_{u,c'}\end{bmatrix}\begin{bmatrix}\mathbf{K}_{\text{Tx1},u,c}\\ \mathbf{K}^*_{\text{Tx2},u,c'}\end{bmatrix} \quad (5)$$

$$\widetilde{\mathbf{\Omega}}_{v,c} = \begin{bmatrix}\mathbf{K}_{\text{Rx1},c} & \mathbf{K}_{\text{Rx2},c}\end{bmatrix}\begin{bmatrix}\mathbf{H}_{v,c} & \mathbf{0}\\ \mathbf{0} & \mathbf{H}^*_{v,c'}\end{bmatrix}\begin{bmatrix}\mathbf{K}_{\text{Tx2},v,c}\\ \mathbf{K}^*_{\text{Tx1},v,c'}\end{bmatrix} \quad (6)$$

where $\widetilde{\mathbf{\Psi}}_{u,c} \in \mathbb{C}^{N\times M_u}$ and $\widetilde{\mathbf{\Omega}}_{v,c} \in \mathbb{C}^{N\times M_v}$. Clearly, (4) includes contribution not only from the desired subcarrier c but also from the image subcarrier c'. The signals transmitted at the image subcarrier c' leak to subcarrier c due to both TX and RX I/Q imbalances and thus we call it *inter-user interference* from the image subcarrier. In contrast to the data signals, the external interference and noise from the image subcarrier c' alias to subcarrier c only due to RX I/Q imbalance. Stemming from the special nature of I/Q imbalance, signals at other subcarriers are not affected.

Note that the special case with I/Q imbalance only in the TX (RX) is obtained from (4) by substituting $\mathbf{K}_{\text{Rx1},c} = \mathbf{I}$ and $\mathbf{K}_{\text{Rx2},c} = \mathbf{0}$ $\forall c$ ($\mathbf{K}_{\text{Tx1},u,c} = \mathbf{I}$ and $\mathbf{K}_{\text{Tx2},u,c} = \mathbf{0}$ $\forall u,c$).

B. Receiver Post-Processing in The Base Station

In MU-MIMO systems the transmitted data streams of different UEs must be eventually separated in the BS while also suppressing any harmful interference effectively. The RX post-processing is implemented by combining the received signals from the RX antennas in a selected manner. When using linear combining, the signals at subcarrier c are post-processed in the digital domain using the combiner weight matrix $\mathbf{W}_c = \left[\mathbf{w}^T_{1,1,c}, \mathbf{w}^T_{1,2,c}, \cdots, \mathbf{w}^T_{Q_U,U,c}\right]^T \in \mathbb{C}^{S\times N}$ where row vector $\mathbf{w}_{q,u,c} \in \mathbb{C}^{1\times N}$ denotes the weights for data stream q of UE u and $S = \sum_{u=1}^{U} Q_u$ is the total amount of the transmitted data streams. Then, the output signal vector $\mathbf{y}_c \in \mathbb{C}^{S\times 1}$ under perfect I/Q matching is given by

$$\mathbf{y}_c = \mathbf{W}_c\mathbf{r}_c = \sum_{u=1}^{U}\mathbf{W}_c\mathbf{H}_{u,c}\mathbf{G}_{u,c}\mathbf{x}_{u,c} + \mathbf{W}_c\mathbf{z}_c. \quad (7)$$

Since the data is processed at the subcarrier level, we call this method per-subcarrier processing. The overall MU-MIMO system with precoded spatial multiplexing is depicted in Fig. 1.

As shown in (4), I/Q imbalance distorts the received antenna signals. Consequently, the combiner output signal under joint

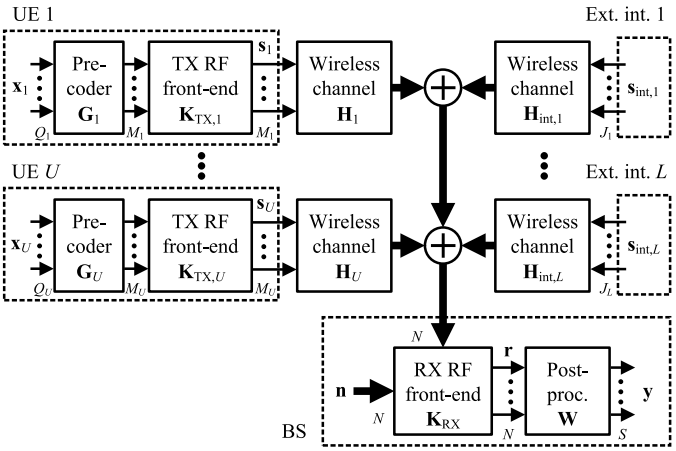

Fig. 1. Illustration of the considered uplink MU-MIMO scenario with devices being active at subcarrier c.

TX+RX I/Q imbalances becomes

$$\begin{aligned}\mathbf{y}_{\text{TxRxi},c} &= \mathbf{W}_c\mathbf{r}_{\text{TxRxi},c}\\ &= \sum_{u=1}^{U}\mathbf{W}_c\widetilde{\mathbf{\Psi}}_{u,c}\mathbf{G}_{u,c}\mathbf{x}_{u,c} + \sum_{v=1}^{V}\mathbf{W}_c\widetilde{\mathbf{\Omega}}_{v,c}\mathbf{G}^*_{v,c'}\mathbf{x}^*_{v,c'}\\ &\quad + \mathbf{W}_c\mathbf{K}_{\text{Rx1},c}\mathbf{z}_c + \mathbf{W}_c\mathbf{K}_{\text{Rx2},c}\mathbf{z}^*_{c'}. \end{aligned} \quad (8)$$

Clearly, the output signal consists of both the desired data streams as well as the interfering UE signals originating from the image subcarrier. In addition, the output signal includes external interference and noise at both subcarriers c and c'. The signal leakage naturally makes the signal separation in the RX more difficult and consequently the overall system performance is also deteriorated, as shown in Section IV.

The signal distortion, where each subcarrier signal is mixed with the signals at the image subcarrier, guides us towards joint post-processing of mirror-subcarriers [6]–[8]. When defining the augmented received signal as $\widetilde{\mathbf{r}}_c = \left[\mathbf{r}^T_c, \mathbf{r}^H_{c'}\right]^T \in \mathbb{C}^{2N\times 1}$, the augmented post-processing is of the form $\widetilde{\mathbf{y}}_c = \widetilde{\mathbf{W}}_c\widetilde{\mathbf{r}}_c$ where the augmented weight matrix $\widetilde{\mathbf{W}}_c = \left[\widetilde{\mathbf{w}}^T_{1,1,c}, \cdots, \widetilde{\mathbf{w}}^T_{Q_U,U,c}\right]^T \in \mathbb{C}^{S\times 2N}$. Now, row vector $\widetilde{\mathbf{w}}_{M_U,U,c} \in \mathbb{C}^{1\times 2N}$ contains separate weights for both subcarrier signals and thus provides more degrees of freedom (DoF) in post-processing.

Under joint TX+RX I/Q imbalances, the augmented combiner output signal $\widetilde{\mathbf{y}}_{\text{TxRxi},c} \in \mathbb{C}^{S\times 1}$ is given by

$$\begin{aligned}\widetilde{\mathbf{y}}_{\text{TxRxi},c} &= \widetilde{\mathbf{W}}_c\widetilde{\mathbf{r}}_{\text{TxRxi},c}\\ &= \sum_{u=1}^{U}\widetilde{\mathbf{W}}_c\widetilde{\mathbf{\Xi}}_{u,c}\mathbf{G}_{u,c}\mathbf{x}_{u,c} + \sum_{v=1}^{V}\widetilde{\mathbf{W}}_c\widetilde{\mathbf{\Phi}}_{v,c}\mathbf{G}^*_{v,c'}\mathbf{x}^*_{v,c'}\\ &\quad + \widetilde{\mathbf{W}}_c\widetilde{\mathbf{K}}_{\text{RxA},c}\mathbf{z}_c + \widetilde{\mathbf{W}}_c\widetilde{\mathbf{K}}_{\text{RxB},c}\mathbf{z}^*_{c'}. \end{aligned} \quad (9)$$

Here, the augmented signal vector under joint TX+RX I/Q imbalances is $\widetilde{\mathbf{r}}_{\text{TxRxi},c} = \left[\mathbf{r}^T_{\text{TxRxi},c}, \mathbf{r}^H_{\text{TxRxi},c'}\right]^T \in \mathbb{C}^{2N\times 1}$ and

the total augmented effective channel matrices are given by

$$\widetilde{\mathbf{\Xi}}_{u,c} = \begin{bmatrix} \mathbf{K}_{\text{Rx1},c} & \mathbf{K}_{\text{Rx2},c} \\ \mathbf{K}^*_{\text{Rx2},c'} & \mathbf{K}^*_{\text{Rx1},c'} \end{bmatrix} \begin{bmatrix} \mathbf{H}_{u,c} & \mathbf{0} \\ \mathbf{0} & \mathbf{H}^*_{u,c'} \end{bmatrix} \begin{bmatrix} \mathbf{K}_{\text{Tx1},u,c} \\ \mathbf{K}^*_{\text{Tx2},u,c'} \end{bmatrix} \quad (10)$$

$$\widetilde{\mathbf{\Phi}}_{v,c} = \begin{bmatrix} \mathbf{K}_{\text{Rx1},c} & \mathbf{K}_{\text{Rx2},c} \\ \mathbf{K}^*_{\text{Rx2},c'} & \mathbf{K}^*_{\text{Rx1},c'} \end{bmatrix} \begin{bmatrix} \mathbf{H}_{v,c} & \mathbf{0} \\ \mathbf{0} & \mathbf{H}^*_{v,c'} \end{bmatrix} \begin{bmatrix} \mathbf{K}_{\text{Tx2},v,c} \\ \mathbf{K}^*_{\text{Tx1},v,c'} \end{bmatrix} \quad (11)$$

where $\widetilde{\mathbf{\Xi}}_{u,c} \in \mathbb{C}^{2N \times M_u}$ and $\widetilde{\mathbf{\Phi}}_{v,c} \in \mathbb{C}^{2N \times M_v}$. Finally, the augmented RX I/Q imbalance matrices, both $\in \mathbb{C}^{2N \times N}$, are

$$\widetilde{\mathbf{K}}_{\text{RxA},c} = \begin{bmatrix} \mathbf{K}_{\text{Rx1},c} \\ \mathbf{K}^*_{\text{Rx2},c'} \end{bmatrix}, \; \widetilde{\mathbf{K}}_{\text{RxB},c} = \begin{bmatrix} \mathbf{K}_{\text{Rx2},c} \\ \mathbf{K}^*_{\text{Rx1},c'} \end{bmatrix}. \quad (12)$$

Despite the similarities between (8) and (9), the underlying capability of the joint subcarrier processing in (9) should be kept in mind. The doubled amount of the weights naturally doubles the computational complexity of the combining process but also enables more flexible post-processing for obtaining the desired signal separation and interference suppression, even under challenging I/Q imbalances. Note that this flexibility is obtained by changing the digital combiner block alone whereas the costly RF chains and demanding FFT processing remain the same as for classical per-subcarrier processing.

III. Precoding and MMSE Post-Processing

Closed-loop type spatial multiplexing can provide significant performance improvements due to the exploitation of known channel state information (CSI) [16]. The spatial signal processing is shared between the TX and RX sides such that the desired link performance is provided. On the TX side, the precoder pre-processes and maps the data streams to the TX antennas. On the RX side, the received antenna signals are post-processed such that different data streams are properly separated while harmful interference is effectively suppressed. In this paper, we assume that perfect uplink CSI for subcarriers c and c', including also the effects of I/Q imbalance, is available for both the UEs as well as the BS. Although this assumption is over-optimistic in practice, we use it for evaluating and demonstrating the performance limits of the closed-loop spatial multiplexing under I/Q imbalance.

A. RF-Aware Precoding

One of the precoding methods is based on singular-value decomposition of the known channel matrix. The singular-value decomposition for the total effective channel matrix of UE u at subcarrier c is given by

$$\widetilde{\mathbf{\Psi}}_{u,c} = \mathbf{U}_{u,c}\mathbf{\Lambda}_{u,c}\mathbf{V}^H_{u,c} \quad (13)$$

where $\mathbf{U}_{u,c} \in \mathbb{C}^{N \times N}$ contains the left singular vectors, $\mathbf{\Lambda}_{u,c} \in \mathbb{C}^{N \times M_u}$ is a diagonal matrix including the singular values, and $\mathbf{V}_{u,c} = \left[\mathbf{v}_{1,u,c}, \mathbf{v}_{2,u,c}, \cdots, \mathbf{v}_{M_u,u,c}\right] \in \mathbb{C}^{M_u \times M_u}$ consists of the right singular vectors. The precoding matrix $\mathbf{G}_{u,c} \in \mathbb{C}^{M_u \times Q_u}$ for UE u, assuming that UE knows only the CSI of its own, at subcarrier c is then obtained as

$$\mathbf{G}_{u,c} = \left[\mathbf{v}_{1,u,c}, \mathbf{v}_{2,u,c}, \cdots, \mathbf{v}_{Q_u,u,c}\right] \quad (14)$$

i.e. the precoder consists of the first Q_u columns of $\mathbf{V}_{u,c}$ [12]. In order to fulfil maximum TX power constraint $P_{\max}$, we need to scale the precoder such that $\text{tr}\left(\mathbf{G}_{u,c}\mathbf{R}_{\text{x},u,c}\mathbf{G}^H_{u,c}\right) \leq P_{\max}$ where $\mathbf{R}_{\text{x},u,c} = \mathbb{E}\left[\mathbf{x}_{u,c}\mathbf{x}^H_{u,c}\right]$ [12]. For simplicity, we assume that the data streams of an individual UE are equal in power. Note that the precoder in (14) adapts the transmission not only to the propagation channel but also to the associated RF front-ends and is therefore called RF-aware precoder.

B. Linear and Augmented Linear MMSE Post-Processing

Spatial post-processing can be implemented in the BS with the well-known LMMSE spatial filter. With the used notation, the LMMSE filter $\mathbf{W}_{\text{LMMSE},c} \in \mathbb{C}^{S \times N}$ is equal to [17]

$$\mathbf{W}_{\text{LMMSE},c} = \left(\mathbf{H}^H_{\text{eff},c}\mathbf{R}^{-1}_{\text{int},c}\mathbf{H}_{\text{eff},c} + \mathbf{R}^{-1}_{\text{x},c}\right)^{-1}\mathbf{H}^H_{\text{eff}}\mathbf{R}^{-1}_{\text{int},c}. \quad (15)$$

Here, $\mathbf{H}_{\text{eff},c} \in \mathbb{C}^{N \times S}$ is the total effective channel matrix consisting of channel responses and precoders of all UEs. Assuming that the total effective CSI including I/Q imbalance is available at the BS, we write

$$\mathbf{H}_{\text{eff},c} = \left[\widetilde{\mathbf{\Psi}}_{1,c}\mathbf{G}_{1,c}, \widetilde{\mathbf{\Psi}}_{2,c}\mathbf{G}_{2,c}, \cdots, \widetilde{\mathbf{\Psi}}_{U,c}\mathbf{G}_{U,c}\right]. \quad (16)$$

In addition, $\mathbf{R}_{\text{x},c} \in \mathbb{C}^{S \times S}$ is the covariance matrix of all the data streams and $\mathbf{R}_{\text{int},c} \in \mathbb{C}^{N \times N}$ is the covariance matrix of the interference and noise. Under joint TX+RX I/Q imbalances $\mathbf{R}_{\text{int},c}$ includes the inter-user interference from c' as well the external interference and noise from both c and c', and is equal to

$$\begin{aligned}\mathbf{R}_{\text{int},c} = &\sum_{v=1}^{V} \sigma^2_{x,v,c'}\widetilde{\mathbf{\Omega}}_{v,c}\mathbf{G}^*_{v,c'}\mathbf{G}^T_{v,c'}\widetilde{\mathbf{\Omega}}_{v,c} \\ &+ \mathbf{K}_{\text{Rx1},c}\mathbf{R}_{\text{z},c}\mathbf{K}^H_{\text{Rx1},c} + \mathbf{K}_{\text{Rx2},c}\mathbf{R}^*_{\text{z},c'}\mathbf{K}^H_{\text{Rx2},c}. \quad (17)\end{aligned}$$

Here, $\mathbf{R}_{\text{z},c} \in \mathbb{C}^{N \times N}$ is given by

$$\mathbf{R}_{\text{z},c} = \mathbb{E}\left[\mathbf{z}_c\mathbf{z}^H_c\right] = \sum_{l=1}^{L} \sigma^2_{\text{int},l,c}\mathbf{H}_{\text{int},l,c}\mathbf{H}^H_{\text{int},l,c} + \sigma^2_{\text{n},c}\mathbf{I} \quad (18)$$

where $\sigma^2_{\text{int},l,c}$ denotes the power of the l^{th} external interferer and $\sigma^2_{\text{n},c}$ denotes the noise power, both at subcarrier c. $\mathbf{R}_{\text{z},c'}$ is obtained from (18) by substituting the subcarrier index c with c'. Note that in principle (17) can be obtained from the CSI and the precoder information of the image subcarrier UEs, and by measuring interference and noise contributions when all UEs at the given cell of the BS are momentarily silent. Finally, assuming that the data streams are independent and equal in power, we get $\mathbf{R}_{\text{x},c} = \sigma^2_{x,c}\mathbf{I}$ where $\sigma^2_{x,c}$ is the power of each data stream.

The above LMMSE spatial equalizer can be used in the RX as such. However, as discussed in Section II.B, the processing capabilities can be enhanced by processing jointly the signal at the image subcarrier. Therefore, we extend the equalizer (15) such that it can process the augmented signal $\widetilde{\mathbf{r}}_{\text{TxRxi},c}$ directly.

The augmented LMMSE equalizer $\widetilde{\mathbf{W}}_{\text{LMMSE},c} \in \mathbb{C}^{S\times 2N}$ is then given by

$$\widetilde{\mathbf{W}}_{\text{LMMSE},c} = \left(\widetilde{\mathbf{H}}_{\text{eff},c}^{H}\widetilde{\mathbf{R}}_{\text{int},c}^{-1}\widetilde{\mathbf{H}}_{\text{eff},c} + \mathbf{R}_{\text{x},c}^{-1}\right)^{-1}\widetilde{\mathbf{H}}_{\text{eff}}^{H}\widetilde{\mathbf{R}}_{\text{int},c}^{-1}. \quad (19)$$

Here, the augmented total effective channel matrix $\widetilde{\mathbf{H}}_{\text{eff},\underline{c}} \in \mathbb{C}^{2N\times S}$ is obtained from (16) by substituting $\widetilde{\mathbf{\Psi}}_{u,c}$ with $\widetilde{\mathbf{\Xi}}_{u,c}$ $\forall u = 1,\cdots,U$. In addition, the augmented covariance matrix of the inter-user interference, external interference and noise is now equal to

$$\widetilde{\mathbf{R}}_{\text{int},c} = \sum_{v=1}^{V}\sigma_{x,v,c'}^{2}\widetilde{\mathbf{\Phi}}_{v,c}\mathbf{G}_{v,c'}^{*}\mathbf{G}_{v,c'}^{T}\widetilde{\mathbf{\Phi}}_{v,c} + \widetilde{\mathbf{K}}_{\text{RxA},c}\mathbf{R}_{\text{z},c}\widetilde{\mathbf{K}}_{\text{RxA},c}^{H} + \widetilde{\mathbf{K}}_{\text{RxB},c}\mathbf{R}_{\text{z},c'}^{*}\widetilde{\mathbf{K}}_{\text{RxB},c}^{H}. \quad (20)$$

The equalizer given by (19) yields the MMSE solution for the augmented linear signal model and thus offers flexible and efficient signal processing solution for I/Q imbalance mitigation as shown in the next section by numerical evaluations.

IV. Numerical Results and Analysis

A. Simulation Settings

In our simulations we consider an uplink OFDMA MU-MIMO scenario with 20 UEs that transmit simultaneously at subcarrier c towards a single BS. Additionally, 20 UEs are communicating with the BS at the image subcarrier c'. In order to illustrate a massive MIMO system, we selected the BS to be equipped with 50 antenna elements. On the UE side, each UE transmits two independent data streams in parallel and the streams are precoded for four antenna elements. At the considered subcarrier as well as at the image subcarrier, we add eight external single-antenna interferers with equal powers to the simulation setup. Furthermore, the signal-to-noise ratio (SNR) in RX branches is set to 30 dB and is here defined as the ratio between the total averaged received signal power originating from all TX branches of a single user, and the noise power. Furthermore, the data streams of the UEs are set to be equal in power. The signal-to-interference ratio (SIR) is here defined as the ratio between the total averaged received signal power of a single UE and the total received power originating from the external interferers.

The spatial channel between the BS array and TX antenna m of UE u is modeled as $\mathbf{h}_{m,u,c} = \mathcal{CN}(\mathbf{0}, \mathbf{R}_{\text{h}})$ where $\mathbf{R}_{\text{h}} = \mathbb{E}[\mathbf{hh}]$ denotes the spatial covariance matrix. We set $\mathbf{R}_{\text{h}}$ according to the exponential correlation model in [5, eq. (17)] with parameters $r = 0.7$ and $\delta = 1$ for modeling highly correlated adjacent antenna elements in the RX which is a fairly common assumption in massive MIMO related work. The channels between the BS and different TX antennas of a single UE as well as between the BS and different UEs are assumed to be uncorrelated.

I/Q imbalance is defined in terms of the image rejection ratio (IRR) which is given in decibels for a single transceiver branch by $\text{IRR} = 10\log_{10}\left(|K_1|^2/|K_2|^2\right)$ [18]. Firstly, the minimum allowable IRR (IRR_{min}) is set to 25 dB which is the minimum requirement for UE TX/RX IRR in the LTE specification [19]. Secondly, we select phase imbalance coefficients $\phi_{\text{Tx},u,m,c}, \forall u,m,c$ and $\phi_{\text{Rx},c,n}, \forall n,c$ independently from $\mathcal{U}(-\alpha,\alpha)$ where α guarantees the selected IRR_{min} when the gain imbalance is set to zero. Finally, the gain imbalance coefficients $g_{\text{Tx},u,m,c}, \forall u,m,c$ and $g_{\text{Rx},c,n}, \forall n,c$ are selected independently from the conditional distribution $\mathcal{U}(g_{\text{min}}, g_{\text{max}})$ where the range edges correspond to IRR_{min} with the earlier selected ϕ. The I/Q imbalance parameters at different subcarriers are assumed to be independent for modeling arbitrarily frequency-selective I/Q imbalance. The default simulation parameters are summarized in Table I while some parameters are also varied in the evaluations.

TABLE I
Baseline simulation parameters

Parameter	Symbol	Value
RX antennas in BS	N	50
Number of UEs	U, V	20
TX antennas in UEs	M_u, M_v	4
Data streams in UEs	Q_u, Q_v	2
Number of external interferers	L_c, $L_{c'}$	8
TX antennas in external interferers	J_l	1
Signal to noise ratio	SNR	30 dB
Signal to interference ratio	SIR_c, $\text{SIR}_{c'}$	-20 dB
Minimum image rejection ratio	IRR_{min}	25 dB

The numerical analysis evaluates the SINR of an arbitrary data stream of an arbitrary UE. Due to the space limitation, the detailed SINR formulations are omitted here but they can be easily calculated based on the signal models in (8) and (9). All the results describe the performance from a single yet arbitrary subcarrier signal point of view, and are averaged over all the data streams, UEs and 1000 realizations. For each realization, the channel responses and I/Q imbalance parameters are randomly and independently generated according to the aforementioned criteria. All figures show the performance for both the LMMSE and the derived augmented LMMSE equalizers.

B. Simulation Results and Discussion

Fig. 2 visualizes the SINR as a function of the number of RX antennas. The results show clearly that the SINR is very low when $N \leq 40$. This is a consequence of the fact that the BS can not separate different data streams and external interference signals due to the lack of DoF. When increasing N, the performance improves steeply when using the augmented equalizer. The SINR improvement gets slower at around 48 antennas which coincides with $N = Q_u U + L$ and means that beyond that point the BS has already enough DoF for data stream separation and interference suppression. In contrast, the per-subcarrier processing yields slower SINR improvement when considering I/Q imbalance in the associated transceiver branches. With TX I/Q imbalance, the performance improves faster than in the other cases. Joint TX+RX imbalances cause the worst performance which suffers heavily from the signal and interference leakage from the image subcarrier. Actually, we see that in this case the LMMSE equalizer needs approximately $N = 80$ antennas to reach the performance which

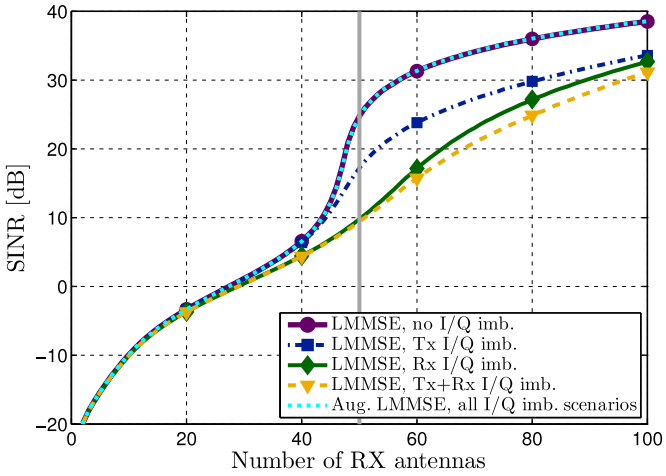

Fig. 2. Average SINR as a function of the number of RX antennas when the other parameters are fixed. The gray vertical line shows the operating point under the conditions given in Table I.

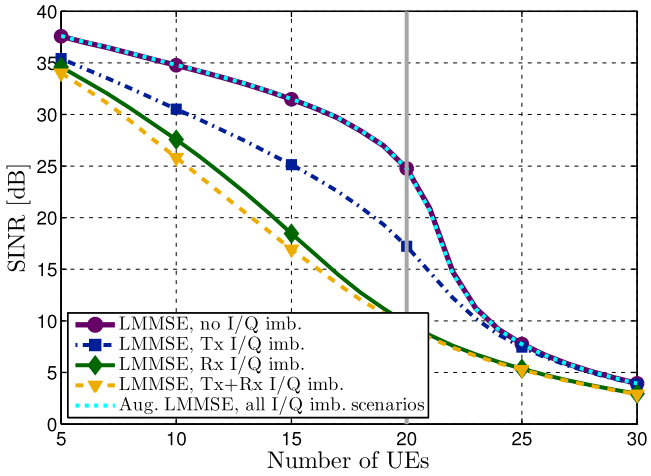

Fig. 3. Average SINR as a function of the number of UEs when the other parameters are fixed. The gray vertical line shows the operating point under the conditions given in Table I.

the augmented processing provides already with 48 antennas. This is an illustrating example of a case where a slight increase in the complexity of digital signal processing can provide big savings in the needed hardware implementation. When increasing N beyond the point where we have enough DoF, RX post-processing can use the excessive resources for noise and interference optimization and thus offer further improvements in the SINR.

Fig. 3 depicts the SINR as a function of the number of UEs. As expected, the performance is good with all the I/Q imbalance scenarios when the BS serves only few UEs. This indicates that massive amount of RX antennas makes the system more robust against I/Q imbalance if (and only if) $N \gg S$. However, with classical linear processing, the SINR deteriorates fast when adding more UEs to the system. This is obviously caused by the increased level of the inter-user interference but also by fewer DoF available for I/Q imbalance mitigation since each additional UE needs additional separation resources in the RX. Again, joint TX+RX I/Q imbalances cause the worst performance which actually degrades very quickly as a function of UEs. This is caused by the signal and interference leakage from the image subcarrier. When considering I/Q imbalance only in the TX, the SINR performance is better since the leakage of the external interference does not occur there. In contrast to the per-subcarrier processing, the derived augmented post-processing provides practically as good performance as with the ideal case and thus outperforms the per-subcarrier processing clearly. This way the overall user capacity of the BS can be increased with changes only in the associated digital signal processing. As the number of UEs goes very high, the BS can not anymore separate different data signals and consequently the performance degrades to low levels in all cases.

Fig. 4 shows the SINR as a function of the number of external interferers. Here, the total interference power is kept constant and consequently the power of individual interferers is decreased when increasing the amount of interferers. Based on the results, the SINR degrades in all cases as L increases since each additional interferer reserves additional spatial resources in the BS. The behavior of the augmented post-processing is somewhat similar to that in Fig. 3 as the total number of incoming signals is essentially swept in both figures. Additionally, the augmented LMMSE equalizer can, again, suppress the harmful effects of I/Q imbalance efficiently. In contrast to this, the performance of the classical per-subcarrier LMMSE equalizer is highly degraded even without any external interferers. This degradation is due to inter-user interference from the image subcarrier which the classical per-subcarrier processing cannot suppress efficiently. This interference is at the highest with joint TX+RX imbalances which consequently result in the worst performance.

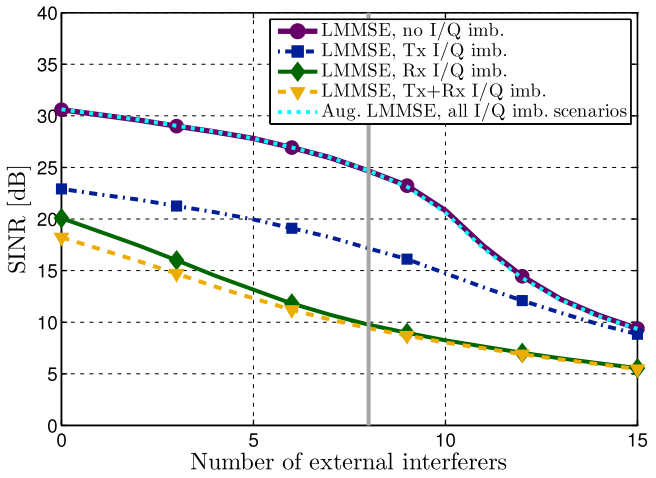

Fig. 4. Average SINR as a function of the number of external interferers when the other parameters are fixed. The gray vertical line shows the operating point under the conditions given in Table I.

Finally, Fig. 5 illustrates the SINR as a function of the minimum allowable IRR. The perfect I/Q matching as well as the augmented equalizer result in a flat SINR performance

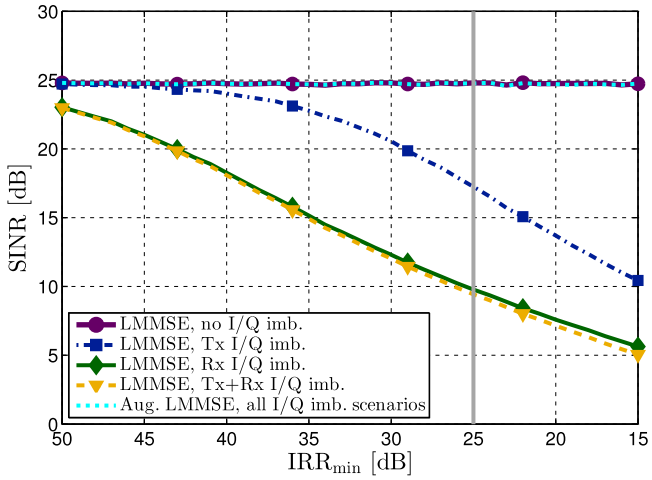

Fig. 5. Average SINR as a function of IRR when the other parameters are fixed. The gray vertical line shows the operating point under the conditions given in Table I.

over varying IRR_{min}. This indicates again that the augmented equalizer can mitigate the harmful effects of I/Q imbalance practically completely and thus allows lower quality for the associated RF components. The per-subcarrier processing suffers big degradations in the SINR. With TX I/Q imbalance, the performance is deteriorated by the inter-user interference from the image subcarrier. RX I/Q imbalance causes also leakage of the external interference and consequently the cases with RX and joint TX+RX imbalances provide the worst performance. Notice that the 25 dB IRR level, which is acceptable in the current LTE specification [19], causes already 8–15 dB SINR degradation.

V. Conclusion

This paper addresses precoded spatial multiplexing in massive MU-MIMO uplink transmission under imperfections in the associated RF circuits. In particular, we formulated and derived the detailed signal models in such scenario, and showed the harmful signal distortion and interference mechanism due to I/Q imbalance in the TX and RX electronics. Stemming from the distortion, where each subcarrier signal is affected also by the signals at the image subcarrier, we exploited so-called augmented spatial equalizer in the BS and derived MMSE-optimal augmented spatial receiver. There, each subcarrier signal is processed jointly with the signal at the image subcarrier, both with separate but jointly optimized sets of weights. Consequently, the available degrees of freedom are doubled while the associated RF chains remain the same as for the linear RX processing. The numerical examples showed that I/Q imbalance heavily deteriorates the performance of the classical per-subcarrier processing. Such performance degradation can be avoided by using the augmented post-processing and the results show that the augmented equalizer is able to reach the same performance as the system with perfect I/Q matchings. Thus the derived augmented spatial equalizer enables the usage of low-cost components in massive MU-MIMO devices without losses in the achievable performance.

References

[1] E. Larsson, O. Edfors, F. Tufvesson, and T. Marzetta, "Massive MIMO for next generation wireless systems," *IEEE Commun. Mag.*, vol. 52, no. 2, pp. 186–195, Feb. 2014.

[2] E. Björnson, M. Matthaiou, and M. Debbah, "Circuit-aware design of energy-efficient massive MIMO systems," in *Proc. Int. Symp. on Commun., Control, and Signal Process. (ISCCSP)*, May 2014. [Online]. Available: http://arxiv.org/abs/1403.4851

[3] A. Hakkarainen, J. Werner, K. R. Dandekar, and M. Valkama, "Widely-linear beamforming and RF impairment suppression in massive antenna arrays," *Journal of Communications and Networks*, vol. 15, no. 4, pp. 383–397, Aug. 2013.

[4] A. Pitarokoilis, S. Mohammed, and E. Larsson, "Effect of oscillator phase noise on uplink performance of large MU-MIMO systems," in *50th Annual Allerton Conference on Communication, Control, and Computing (Allerton)*, Oct. 2012, pp. 1190–1197.

[5] E. Björnson, J. Hoydis, M. Kountouris, and M. Debbah, "Massive MIMO systems with non-ideal hardware: Energy efficiency, estimation, and capacity limits," *IEEE Trans. Inf. Theory*, 2013, submitted. [Online]. Available: http://arxiv.org/abs/1307.2584

[6] A. Tarighat and A. Sayed, "MIMO OFDM receivers for systems with IQ imbalances," *IEEE Trans. Signal Process.*, vol. 53, no. 9, pp. 3583–3596, Sep. 2005.

[7] A. Tarighat, R. Bagheri, and A. Sayed, "Compensation schemes and performance analysis of IQ imbalances in OFDM receivers," *IEEE Trans. Signal Process.*, vol. 53, no. 8, pp. 3257–3268, Aug. 2005.

[8] O. Özdemir, R. Hamila, and N. Al-Dhahir, "I/Q imbalance in multiple beamforming OFDM transceivers: SINR analysis and digital baseband compensation," *IEEE Trans. Commun.*, vol. 61, no. 5, pp. 1914–1925, May 2013.

[9] A. Hakkarainen, J. Werner, K. R. Dandekar, and M. Valkama, "Analysis and augmented spatial processing for uplink OFDMA MU-MIMO receiver under transceiver I/Q imbalance and external interference," *IEEE Trans. Wireless Commun.*, 2014, submitted. [Online]. Available: http://arxiv.org/abs/1407.0524

[10] S. Mirabbasi and K. Martin, "Classical and modern receiver architectures," *IEEE Commun. Mag.*, vol. 38, no. 11, pp. 132–139, Nov. 2000.

[11] T. Schenk, *RF Imperfections in High-rate Wireless Systems: Impact and Digital Compensation*, 1st ed. Springer, 2008.

[12] D. P. Palomar and Y. Jiang, "MIMO transceiver design via majorization theory," *Foundations and Trends in Communications and Information Theory*, vol. 3, no. 4-5, pp. 331–551, 2006.

[13] D. Tandur and M. Moonen, "Joint adaptive compensation of transmitter and receiver IQ imbalance under carrier frequency offset in OFDM-based systems," *IEEE Trans. Signal Process.*, vol. 55, no. 11, pp. 5246–5252, Nov. 2007.

[14] F.-L. Luo, *Digital Front-End in Wireless Communications and Broadcasting: Circuits and Signal Processing*. Cambridge University Press, Sep. 2011.

[15] O. Özdemir, R. Hamila, and N. Al-Dhahir, "Exact SINR analysis of OFDM systems under joint Tx/RX I/Q imbalance," in *Proc. IEEE PIMRC*, 2013, pp. 646–650.

[16] H. Sampath, P. Stoica, and A. Paulraj, "Generalized linear precoder and decoder design for MIMO channels using the weighted MMSE criterion," *IEEE Trans. Commun.*, vol. 49, no. 12, pp. 2198–2206, Dec. 2001.

[17] S. Bittner, W. Rave, and G. Fettweis, "Phase noise suppression in OFDM with spatial multiplexing," in *Proc. IEEE VTC-Spring*, Apr. 2007, pp. 1826–1830.

[18] L. Anttila, M. Valkama, and M. Renfors, "Circularity-based I/Q imbalance compensation in wideband direct-conversion receivers," *IEEE Trans. Veh. Technol.*, vol. 57, no. 4, pp. 2099 –2113, Jul. 2008.

[19] *Evolved Universal Terrestrial Radio Access (E-UTRA); User Equipment (UE) radio transmission and reception*, The 3rd Generation Partnership Project (3GPP), Techical Specification 36.101 v. 11.8.0, Mar. 2014.